JACS ARTICLES

Published on Web 05/25/2010

# The Protease-Mediated Nucleus Shuttles of Subnanometer Gold Quantum Dots for Real-Time Monitoring of Apoptotic Cell Death

Shu-Yi Lin,[†,§] Nai-Tzu Chen,[‡,||] Shu-Pin Sun,[‡] Jerry C. Chang,[‡] Yu-Chao Wang,[†] Chung-Shi Yang,[*,†,§] and Leu-Wei Lo[*,‡]

*Center for Nanomedicine Research and Division of Medical Engineering Research, National Health Research Institutes, 35 Keyan Road Zhunan, Miaoli, Taiwan, 350, Department of Applied Chemistry and Graduate Institute of Biomedicine and Biomedical Technology, National Chi-Nan University, Puli, Taiwan, 545, and Department of Chemistry, National Taiwan University, Taipei, Taiwan, 106*

Received January 21, 2010; E-mail: lwlo@nhri.org.tw; cyang@nhri.org.tw

***Abstract:*** Subnanometer photoluminescent gold quantum dots (GQDs) are functionalized with a peptide moiety that contains both nuclear export signal (NES) and nuclear localization signal (NLS) sequences. By taking advantage of its small size and great photostability, the functionalized GQDs are used to mimic the actions of nucleus shuttle proteins, especially of those activated during cell apoptotic death, to work as protease-mediated cytoplasm−nucleus shuttles for dynamic monitoring of apoptosis. The resulting construct demonstrates activation of the nuclear pore complex (NPC) of cells, for bidirectional transport between nucleus and cytoplasm. A capsase-3 recognition sequence (DEVD), placed within the NLS/NES peptide, serves as a proteolytic site for activated caspase-3. Upon the induction of apoptosis, the activated caspase-3 cleaves the functional peptide on GQDs resulting in changes of subcellular distribution of GQDs. Such changes can be quantified as a function of time, by the ratios of GQDs photoluminescence in nucleus to that in cytoplasm. As such, the NES-linker-DEVD-linker-NLS peptide enables the GQDs to function as molecular probes for the real-time monitoring of cellular apoptosis.

## Introduction

Apoptosis, the process of programmed cell death, is controlled by a wide variety of intracellular and extracellular factors. Among apoptotic effector proteases, caspase-3 has been identified as being a key mediator of the execution phase of apoptosis of mammalian cells.[1,2] Consequently, assays of caspase-3 activation have been used widely for the *in vitro* detection of apoptosis. Most of these assays, however, are performed using cell extracts from a population of cells on apoptotic progression. With the advance of genetic-engineered probes, several studies acquiring the dynamics of caspase-3 activation have been reported. For example, the dynamics of activated caspase-3 in living cells by fluorescence resonance energy transfer (FRET) of targeted fusion proteins has been reported.[2−4] The performance of FRET-based sensors was mainly dependent on the efficiency of energy transfer between the fluorescence donor and acceptor. In addition, Kanno et al. developed a genetically encoded cyclic luciferase and demonstrated its efficient applicability in real-time analysis of caspase-3 activity in living cells and animals by turning on/off of the bioluminescent reporter.[5]

Another important category of approach for sensing cellular events is the nanoparticle-mediated sensors, where the particle materials, size, and surface characteristics are playing determinant roles. Among others, gold nanoparticles (GNPs) including nanospheres and nanorods that measured in the tens of nanometers hold great promises in tumor therapy and drug delivery, due to their ability to serve as biocompatible scaffolds for intracellular targeting.[6−13] GNPs modified with various small biomolecules such as peptides have been reported to facilitate

[†] Center for Nanomedicine Research, National Health Research Institutes.
[§] National Chi-Nan University.
[‡] Division of Medical Engineering Research, National Health Research Institutes.
[||] National Taiwan University.

(1) Green, D. R. *Cell* **1998**, *94*, 695–698.
(2) Luo, K. Q.; Yu, V. C.; Pu, Y.; Chang, D. C. *Biochem. Biophys. Res. Commun.* **2001**, *283*, 1054–1060.
(3) Elphick, L. M.; Meinander, A.; Mikhailov, A.; Richard, M.; Toms, N. J.; Eriksson, J. E.; Kass, G. E. N. *Anal. Biochem.* **2006**, *349*, 148–155.
(4) Bruns, T.; Angres, B.; Steuer, H.; Weber, P.; Wagner, M.; Schneckenburger, H. *J. Biomed. Opt.* **2009**, 14.
(5) Kanno, A.; Yamanaka, Y.; Hirano, H.; Umezawa, Y.; Ozawa, T. *Angew. Chem., Int. Ed.* **2007**, *46*, 7595–7599.
(6) Paciotti, G. F.; Myer, L.; Weinreich, D.; Goia, D.; Pavel, N.; McLaughlin, R. E.; Tamarkin, L. *Drug Delivery* **2004**, *11*, 169–183.
(7) Cuenca, A. G.; Jiang, H. B.; Hochwald, S. N.; Delano, M.; Cance, W. G.; Grobmyer, S. R. *Cancer* **2006**, *107*, 459–466.
(8) Huang, X. H.; El-Sayed, I. H.; Qian, W.; El-Sayed, M. A. *J. Am. Chem. Soc.* **2006**, *128*, 2115–2120.
(9) Paciotti, G. F.; Kingston, D. G. I.; Tamarkin, L. *Drug Dev. Res.* **2006**, *67*, 47–54.
(10) Gibson, J. D.; Khanal, B. P.; Zubarev, E. R. *J. Am. Chem. Soc.* **2007**, *129*, 11653–11661.
(11) Eghtedari, M.; Liopo, A. V.; Copland, J. A.; Oraevsky, A. A.; Motamedi, M. *Nano Lett.* **2009**, *9*, 287–291.
(12) Qian, X. M.; Peng, X. H.; Ansari, D. O.; Yin-Goen, Q.; Chen, G. Z.; Shin, D. M.; Yang, L.; Young, A. N.; Wang, M. D.; Nie, S. M. *Nat. Biotechnol.* **2008**, *26*, 83–90.

  

their intracellular targeting via receptor-mediated endocytosis (RME).[14−19] Intracellular tracking of the targeted GNPs is typically achieved by labeling particles with visible fluorescence dyes, which however demonstrated insufficient contrast in imaging, mainly due to GNPs which are inherently fluorescence quenchers.[20−24] A nonfluorescent probe using GNPs has also been developed to observe early stage caspase-3 activation in live cells.[25] Such a probe, so-called "plasmon ruler", composed of a core particle surrounded by GNP satellites linked via specific-peptide with the capsase-3 recognition sequence (DEVD), allows continuously imaging trajectories of caspase-3 activity in live cells.[25] In the present study, unlike GNPs, we synthesized subnanometer photoluminescent gold quantum dots (GQDs) as nucleus shuttles and functionalized their surfaces with peptides that recognize activated caspase-3, to enable the real-time monitoring of cellular apoptosis.

Of critical importance to the design of an apoptosis-sensing nucleus shuttle is the nucleus transport efficiency of the nanoparticle. The process of nuclear pore complex (NPC) activation and transportation for nucleo-cytoplasmic exchange is size dependent, with a cutoff at approximately 40 nm.[26] GNPs with 20 nm diameters and functionalized with peptides that contain SV40 NLS have demonstrated efficient nuclear targeting capability; especially when compared to larger GNPs.[14−16,18] However, any surface functionalization of nanoparticles invariably increases their hydrodynamic diameters, and thus further impedes their efficiency of nuclear transportation.[15,27] The 1 to 2 order-of-magnitude smaller size of GQDs circumvents the NPC's size constraint in large measure, and thus enables easier activation of nuclear transport after surface anchorage of targeting peptides. Recently, Lin et al. illustrated the feasibility of using GQDs functionalized with SV40 NLS to activate the NPC transportation, for nucleus targeting and intracellular imaging.[28]

GQDs are composed of only a few to 10 atoms and generally have subnanometer diameters compared to GNPs.[29−31] More importantly, GQDs possess strong photoluminescence that can be exploited for tracking subcellular distributions without the additional difficulties associated with fluorophore conjugation.[28] Subnanometer GQDs are smaller than most of the nuclear proteins (e.g., RNA polymerases) that are first synthesized within cytoplasm and then unidirectionally transported into the nucleus by association with NLS.[28] Several nuclear proteins, such as heterogeneous nuclear ribonucleoprotein A1 and exportin, can repeatedly shuttle in and out of the NPC while in association with specific signaling proteins that bear NLS and the nuclear-export signal (NES).[32] There are also reports indicating that human serine/theronine kinase, mammalian STE20-like kinase (MST), such as Mst3, translocates into the nucleus during apoptosis.[33,34] Upon the basis of the signal-transduction, pathway-driven schema of NPC transport, we mimic the actions of nucleus shuttle proteins by functionalizing the GQDs with a peptide moiety that contains both the lysine-rich NLS and leucine-rich NES, to implement a cytoplasm−nucleus shuttle of GQDs (Figure 1a). The subnanometer GQDs functionalized with NLS and NES possess size and molecular weight (7.2 kDa) much smaller than those of nucleus shuttle proteins like Mst3 (102 kDa) activated upon caspase-mediated apoptosis.

The GQDs are delivered into the cell and nucleus by the leading NLS and then shuttled out of the nucleus by the counteractive NES of the peptide moiety. The GQDs eventually reach equilibrium of subcellular distribution, between cytoplasm and nucleus, as a result of the synergic effects of NLS and NES. To continuously monitor cell apoptosis, the proteolytic moiety DEVD (Asp-GLu-Val-Asp)-peptide sequence is strategically placed between the NES and NLS, to produce the apoptotic-sensing probe of GQD-NES-linker-DEVD-linker-NLS. The DEVD sequence is the proteolytic site of activated caspase-3.[35] During apoptosis, the activated caspase-3 proteolytically cleaves the DEVD-linker-NLS moiety from the remaining GQDs-NES, enabling the GQDs exported from the nucleus to remain residing in the cytoplasm. Consequently, the photoluminescence of GQDs within the nucleus gradually diminishes during apoptosis from its preapoptotic maximum at equilibrium (Figure 1b). Hence, the GQDs-NES-linker-DEVD-linker-NLS complex functions as a molecular probe of the execution phase of cellular apoptosis, as mediated by the caspase-3.

## Experimental Section

**Synthesis and Conjugation of Gold Quantum Dots.** All chemicals were purchased from Sigma-Aldrich. All glassware was thoroughly washed with freshly preparedly 3:1 $HCl/HNO_3$ (aqua regia) and rinsed with Millipore-Q water prior to use. To synthesize gold quantum dots (GQDs) with subnanometer diameters, gold ions


(13) Sperling, R. A.; Gil, P. R.; Zhang, F.; Zanella, M.; Parak, W. J. *Chem. Soc. Rev.* **2008**, *37*, 1896–1908.
(14) Tkachenko, A. G.; Xie, H.; Coleman, D.; Glomm, W.; Ryan, J.; Anderson, M. F.; Franzen, S.; Feldheim, D. L. *J. Am. Chem. Soc.* **2003**, *125*, 4700–4701.
(15) Tkachenko, A. G.; Xie, H.; Liu, Y. L.; Coleman, D.; Ryan, J.; Glomm, W. R.; Shipton, M. K.; Franzen, S.; Feldheim, D. L. *Bioconjugate Chem.* **2004**, *15*, 482–490.
(16) de la Fuente, J. M.; Berry, C. C. *Bioconjugate Chem.* **2005**, *16*, 1176–1180.
(17) Bergen, J. M.; von Recum, H. A.; Goodman, T. T.; Massey, A. P.; Pun, S. H. *Macromol. Biosci.* **2006**, *6*, 506–516.
(18) Oyelere, A. K.; Chen, P. C.; Huang, X.; El-Sayed, I. H.; El-Sayed, M. A. *Bioconjugate Chem.* **2007**, *18*, 1490–1497.
(19) Stewart, K. M.; Horton, K. L.; Kelley, S. O. *Org. Biomol. Chem.* **2008**, *6*, 2242–2255.
(20) Kuo, C. W.; Lai, J. J.; Wei, K. H.; Chen, P. *Adv. Funct. Mater.* **2007**, *17*, 3707–3714.
(21) Verma, A.; Uzun, O.; Hu, Y. H.; Hu, Y.; Han, H. S.; Watson, N.; Chen, S. L.; Irvine, D. J.; Stellacci, F. *Nat. Mater.* **2008**, *7*, 588–595.
(22) Zhang, G. D.; Yang, Z.; Lu, W.; Zhang, R.; Huang, Q.; Tian, M.; Li, L.; Liang, D.; Li, C. *Biomaterials* **2009**, *30*, 1928–1936.
(23) Dulkeith, E.; Morteani, A. C.; Niedereichholz, T.; Klar, T. A.; Feldmann, J.; Levi, S. A.; van Veggel, F.; Reinhoudt, D. N.; Moller, M.; Gittins, D. I. *Phys. Rev. Lett.* **2002**, *89*, 203002.
(24) Dulkeith, E.; Ringler, M.; Klar, T. A.; Feldmann, J.; Javier, A. M.; Parak, W. J. *Nano Lett.* **2005**, *5*, 585–589.
(25) Jun, Y. W.; Sheikholeslami, S.; Hostetter, D. R.; Tajon, C.; Craik, C. S.; Alivisatos, A. P. *Proc. Natl. Acad. Sci. U.S.A.* **2009**, *106*, 17735–17740.
(26) Pante, N.; Kann, M. *Mol. Biol. Cell* **2002**, *13*, 425–434.
(27) Krueger, K. M.; Al-Somali, A. M.; Mejia, M.; Colvin, V. L. *Nanotechnology* **2007**, *18*, 475709.
(28) Lin, S. Y.; Chen, N. T.; Sum, S. P.; Lo, L. W.; Yang, C. S. *Chem. Commun.* **2008**, 4762–4764.
(29) Zheng, J.; Zhang, C.; Dickson, R. M. *Phys. Rev. Lett.* **2004**, *93*, 077402.
(30) Bao, Y. P.; Zhong, C.; Vu, D. M.; Temirov, J. P.; Dyer, R. B.; Martinez, J. S. *J. Phys. Chem. C* **2007**, *111*, 12194–12198.
(31) Liu, X. F.; Li, C. H.; Xu, J. L.; Lv, J.; Zhu, M.; Guo, Y. B.; Cui, S.; Liu, H. B.; Wang, S.; Li, Y. L. *J. Phys. Chem. C* **2008**, *112*, 10778–10783.
(32) Lodish, H.; Berk, A.; Zipursky, S. L.; Matsudaira, P.; Baltimore, D.; Darnell, J. , *Molecular Cell Biology*; W. H. Freeman and Company: New York, 2000.
(33) Lee, K. K.; Ohyama, T.; Yajima, N.; Tsubuki, S.; Yonehara, S. *J. Biol. Chem.* **2001**, *276*, 19276–19285.
(34) Lee, W. S.; Hsu, C. Y.; Wang, P. L.; Huang, C. Y. F.; Chang, C. H.; Yuan, C. J. *FEBS Lett.* **2004**, *572*, 41–45.
(35) Xu, X.; Gerard, A. L. V.; Huang, B. C. B.; Anderson, D. C.; Payan, D. G.; Luo, Y. *Nucleic Acids Res.* **1998**, *26*, 2034–2035.

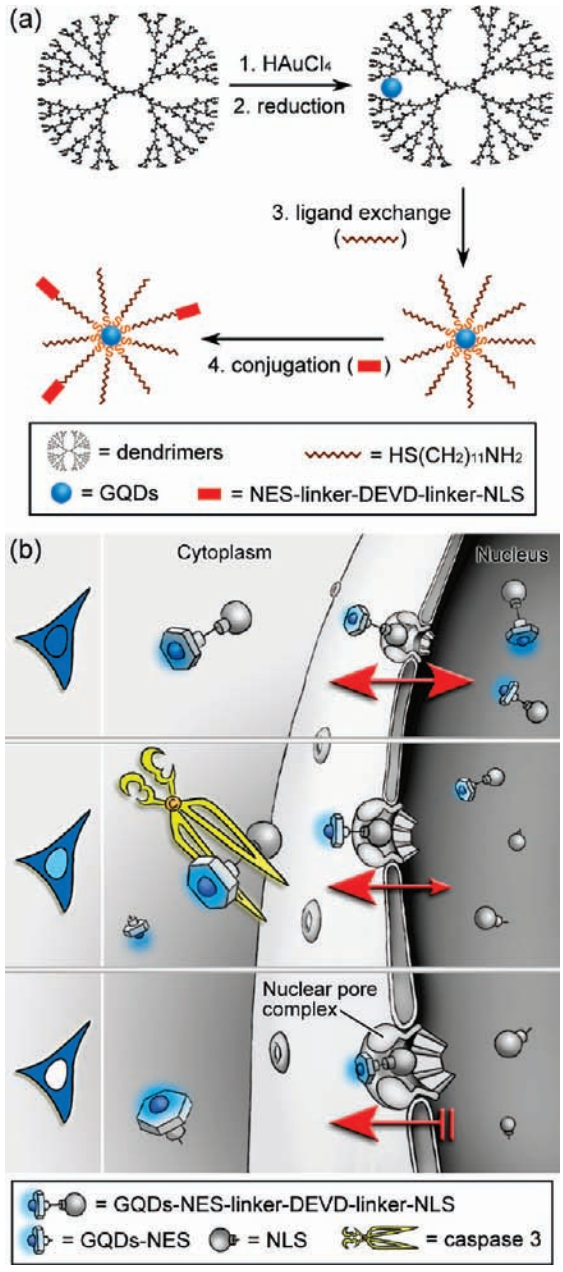


***Figure 1.*** (a) Illustration of GQD synthesis and derivatization. (b) Schematic representation of the nucleus shuttle of GQDs functionalized with the peptide moiety containing NLS, NES and the caspase-3 responsive DEVD that allow monitoring of cell apoptotic progression.

(10 wt % in aqua regia 1.5 $\mu$mol) were added to 5 mL of water (18 M$\Omega$ cm$^{-1}$) containing hydroxyl-terminated polyamidoamine (PAM-AM, 10 wt % in methanol, 0.25 $\mu$mol). The solution was then stirred in a cold room (4 °C) for 24 h until its color transformed from pale yellow to blue, and then shaken at 37 °C for 3 days. Ligand exchange of GQDs proceeded by adding 11-amino-1-undecanethiol (20 mM in ethanol, 20 $\mu$L) to GQD aqua and stirring in darkness for 2 days. Excess thiols were excluded from GQD aqua by dialysis. The AUAT-GQDs were then lyophilized and stored in darkness. In the subsequent peptide conjugation step, excess amounts of EDC (10 equiv) and peptide (3 equiv) were added to the GQDs (1 equiv) aqueous suspension, and mixed at room temperature for 2 days. The final product was lyophilized after dialysis in deionized water for three cycles. The measured quantum yield of GQDs was approximately 6%.

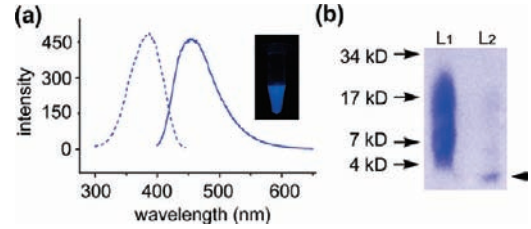


***Figure 2.*** (a) The photoluminescent spectra of GQDs capped with thiol-terminated molecules. The excitation (dashed line) and emission (solid line) indicate the peaks are at 390 and 455 nm, respectively. Inset is a white-light photograph of the GQDs soultion. (b) The SDS-PAGE illustrates the distributions of molecular weights notched with protein markers, before and after the GQDs-NES-linker-DEVD-linker-NLS were mixed with caspase-3 (as shown in lanes $L_1$ and $L_2$, respectively). Note the SDS-PAGE was staining peptides with coomassie blue. The bold arrow on the right marks the molecular weight of 2 kDa, where the appeared band in lane L2 can be referred to the proteolytically cleaved peptide moiety (DEVD-link-NLS).

**Cellular Uptake.** HeLa cells were cultured in a humidified atmosphere with 5% $CO_2$. The cell culture medium was Minimum Essential Medium (MEM; Gibco) supplemented with 10% fetal bovine serum (FBS; Hyclone). For confocal microscopy, cells were plated 24 h before each experiment. After incubation with GQD or GQD-peptides for 1.5 h, cells were stained with the nucleus-specific dye SYTO 59. Images were captured by a Leica TCS confocal spectral microscope using 63× oil immersion objective. Quantitative ratios of photoluminescence intensity per image pixel of GQD-peptides for each condition were quantified by the MetaMorph image analysis software based on four independent confocal microscopic measurements. The average ratio of photoluminescence intensity/pixel of neclues ($I_{nucleus}$) to that of cell ($I_{cell}$) was calculated based on the region of interest (ROI) selected under phase contrast image of cell and fluorescence image of SYTO. The ROI of nucleus at the late stage of apoptosis was defined following the nuclear membrane that envelops the condensed DNA, as delineated in Kihlmark et al.[36]

**Flow Cytometry.** Cells were treated with Staurosporine (S5921, Sigma-Aldrich) at 0.1 and 4 $\mu$M in MEM medium, respectively, and then incubated at 37 °C, 5% $CO_2$(g) for 0, 1, 2, 4, 6, and 8 h. Cells were then centrifuged at 1200 rpm for 5 min. Cell apoptosis was assessed by APO-DIRECTTM Flow Cytometry kit (APT110, Chemicon) using a flow cytometer equipped with a 488 nm argon laser. Propidium iodide and Fluorescein were used to stain DNA and apoptotic cells, respectively. Dual-channel fluorescence analysis enabled both determination of the number of apoptotic cells at a particular cell cycle stage (at least 1 × $10^4$ cells per each measurement) and subsequent flow cytometric analysis using the FSC/FL2 profile. All flow cytometric analyses were performed on FACS Calibur (BD PharMingen) using Cellquest analysis software.

**Western Blotting.** Cells were treated with Staurosporine (S5921, Sigma) at 4 $\mu$M in MEM medium and incubated at 37 °C, 5% $CO_2$(g) for 0, 2, 4, 6, and 8 h. Cells were centrifuged at 1200 rpm for 5 min. The cell pellet was resuspended in a lysis buffer (20 mM HEPES; 20% (w/v) glycerol, 500 mM NaCl, 1.5 mM $MgCl_2$, 0.2 mM EDTA, 1 mM DTT; 0.1% (w/v) Triton X-100) and a protease inhibitor cocktail (K268-50, 1:500, BioVision) at 4 °C for 1 h. Cell homogenates were then centrifuged at 12 000 rpm and 4 °C for 10 min. Protein content was determined with a Bio-Rad Protein Assay (500-0006, Bio-Rad). Equal amounts of protein (50 $\mu$g) were loaded onto SDS−polyacrylamide gels (12%), separated at 100 V for 2 h, and then blotted to PVDF membranes (IPVH00010, Millipore) in transfer buffer (25 mM Tris, 192 mM glycine, and 0.1% SDS) at 250 mA for 100 min. The blots were blocked with 5% nonfat dry milk in TBST (138 mM NaCl, 2.7

(36) Kihlmark, M.; Imreh, G.; Hallberg, E. *J. Cell Sci.* **2001**, *114*, 3643–3653.

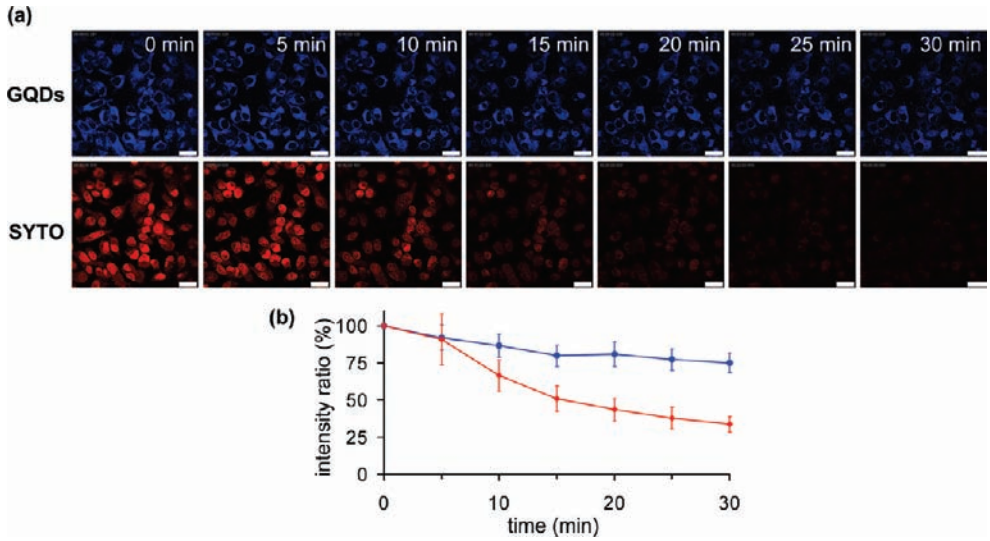


***Figure 3.*** (a) The time-dependent confocal images of HeLa cells pretreated with GQDs capped with thiol-terminated molecules vs SYTO, an organic fluorescent dye used for nuclear staining. The scale bars are 25 $\mu$m. Note that all of the confocal images were equally corrected for brightness. (b) The intensity ratios of both GQDs capped with thiol-terminated molecules (blue line) and SYTO (red line) to their image backgrounds vs time are calculated, indicating a better resistance of photobleaching rendered by GQDs as compared to SYTO.

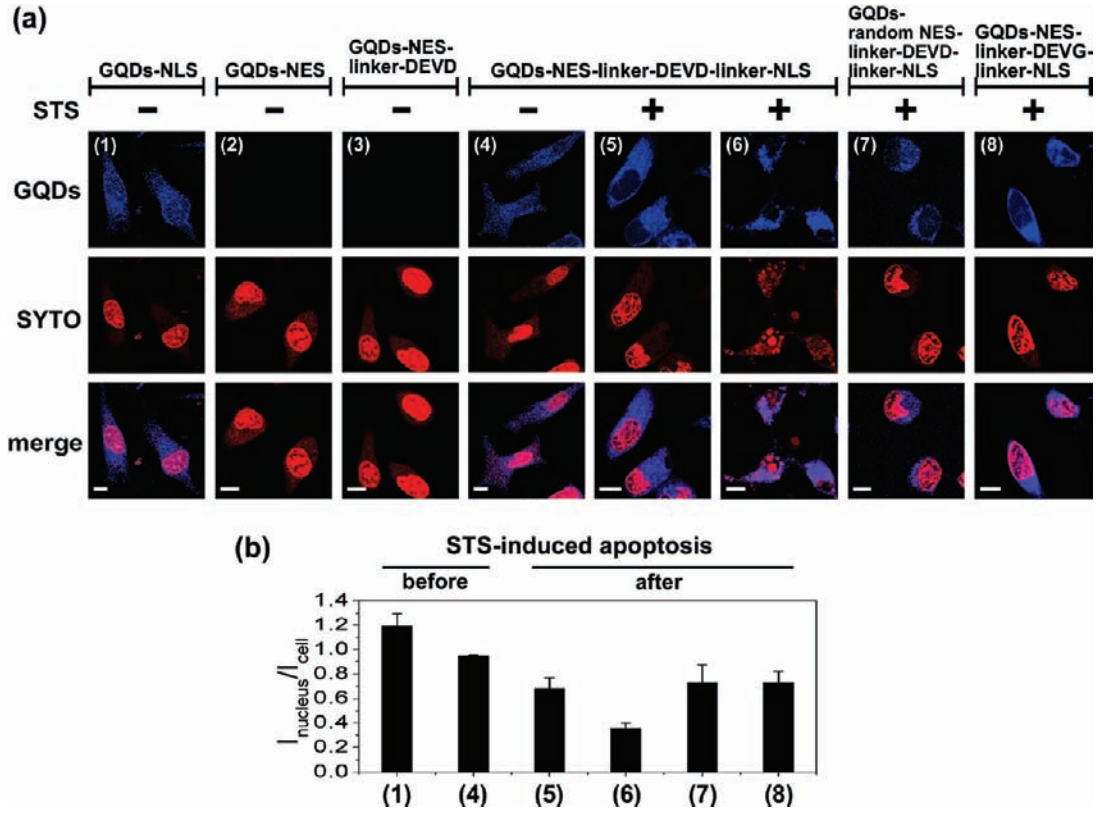


***Figure 4.*** (a) Confocal microscopic images show the GQDs' exportation of the nucleus in response to the STS-induced cell apoptosis. The control groups include HeLa cells incubated with the GQDs-NLS (column 1), the GQDs-NES (column 2), the GQDs-NES-linker-DEVD (column 3), and the GQDs-NES-linker-DEVD-linker-NLS (column 4) for 1.5 h, respectively. After incubation with the GQDs-NES-linker-DEVD-linker-NLS (columns 5 and 6), GQDs-random-NES-linker-DEVD-linker-NLS (column 7) and GQDs-NES-linker-DEVG-linker-NLS (column 8), apoptosis of HeLa cells was subsequently induced by treating the cells with STS (0.1 $\mu$M) for 1 h (column 5) and STS (4 $\mu$M) for 4 h (columns 6−8). Scale bar: 10 $\mu$m. SYTO: a specific dye for nuclear staining. (b) Quantitative ratios of photoluminescence intensity of GQDs observed in nucleus vs that in cell. The ratios decrease after the induction of apoptosis, indicating the predominance of GQDs exportation from the nucleus. The ratio for each condition was quantified by the MetaMorph image analysis software based on four independent confocal microscopic measurements.

mM KCl, pH 7.5, and 0.1% Tween 20) at room temperature for 2 h. Membranes were incubated as follows: a rabbit polyclonal to active+pro caspase-3 antibody (ab47131, 1:2000, abcam); a rabbit polyclonal to $\beta$-tubulin antibody (NB600-936; 1:10 000, Novus Biologicals). Membranes were washed with PBST four times for 60 min and incubated with anti-rabbit peroxidase-conjugated secondary antibodies (111-035-003, Jackson Immuno Research) for 1 h. Blots were washed and developed using an ECL chemiluminescence detection reagent (Amersham Biosciences). Membranes were stripped in Re-Blot Plus Strong Antibody Stripping Solution

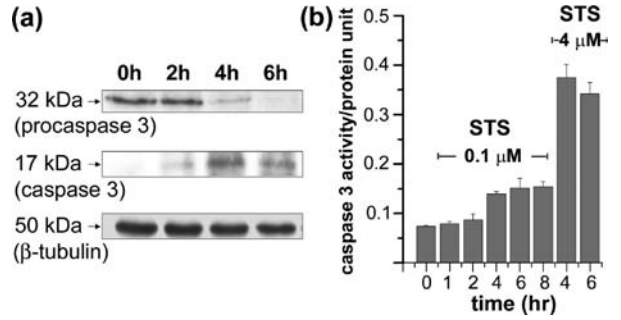


***Figure 5.*** (a) Western blot analysis of the active caspase-3 expression following STS-induced cell apoptosis. Pro-caspase-3 (32 kDa) and its downstream active caspase-3 (17 kDa) were analyzed in whole cell protein extracts. α-Tubulin (50 kDa) serves as an internal control for protein loading. (b) The histogram presents caspase-3 activity induced by STS is both concentration- and time-dependent.

(2504, Chmicon) at room temperature for 20 min, washed three times in TBST for 45 min, and then reprobed.

**Analysis of Caspase-3 Activity.** Caspase-3 activity was detected by use of the caspase-3 Colorimetric Activity Assay Kit (Chemicon). Briefly, HeLa cells were seeded into 35 mm plates at $1 \times 10^5$ cells/well. After being exposed to low (0.1 $\mu$M) or high (4 $\mu$M) concentration of staurosporine (STS) for a fixed time (0, 1, 2, 4, 6, 8 h), cells were washed with PBS and retrieved by harvest solution (40 mM Tris-HCl, pH 7.4, 1 mM EDTA, and 150 mM NaCl). Cell lysate was extracted using lysis buffer (PBS + 0.1% NP-40) and protein content of protein was determined by the BIO-RAD Bradford protein assay. For each well in a 96 well microplate, cell lysate (70 $\mu$L), assay buffer (20 $\mu$L), and caspase-3 substrate (Ac-DEVD-pNA, 10 $\mu$L) were combined. The samples were then incubated at 37 °C for 2 h and then characterized with a microtiter plate reader operating at a wavelength of 405 nm.

## Results and Discussion

GQDs were synthesized using a method based on polyamidoamine (PAMAM) dendrimer encapsulation reported previously by us,[28] but with thiol-terminated amines used as connecting ligands for conjugating the peptide moieties to the GQDs. The maximal excitation and emission wavelengths of GQD photoluminescence were 390 and 455 nm, respectively (Figure 2a), consistent with previously reported results[28,30] and indicative of $Au_8$ atomic clusters, based on the spherical Jellium model.[29] Transmission IR spectra (data not shown) displayed the disappearance of SH signature (2550 $cm^{-1}$) and the appearance of 1645 and 1554 $cm^{-1}$ stand for amine, indicating the thiol-terminated ligand exchange of dendrimers. Because of the subnanometer size for GQD, the number of ligand and the ligand bound to peptide per GQD was difficult to be estimated. Nevertheless, it should be less than the number of ligands per GQD. Synthesized GQDs can accommodate as many as eight thiol-terminated molecules, when the GQDs comprise fewer than 10 gold atoms.[37] Since the size of peptide domain is far larger than that of GQD's diameter (average diameter <1 nm), the final number of peptide functionalized on every GQD should be less than eight.[38] The estimation was further verified via the *in vitro* proteolytic cleavage experiments of GQDs-NES-linker-DEVD-linker-NLS by caspase-3. SDS-PAGE revealed peptide bands between 7 and 17 kDa before treating the functionalized GQDs with caspase-3 (Figure 2b, L1). Such a distribution of molecular weights indicated the number of peptide conjugation on the surface of GQDs was in the range of 1−5 (corresponding to molecular weight: 7.2−20 kDa). After mixing with the caspase-3, the SDS-PAGE of GQDs-NES-linker-DEVD-linker-NLS illustrated a distinct band with much lower molecular weight (ca. 2 kDa) (Figure 2b, L2). This molecular weight was referred to the peptide moiety (DEVD-link-NLS) which was proteolytically cleaved from the GQDs-NES-linker-DEVD-linker-NLS by caspase-3. Nevertheless, even with less than eight NES-linker-DEVD-linker-NLS peptides per GQD, our later *in vitro* studies (Figure 4) demonstrated the functionalized GQDs to be efficiently shuttled across the nuclear membrane of HeLa cells responding to staurosporine (STS)-induced apoptosis.

Not only does the subnanometer of size facilitate the GQDs work as the nucleus shuttles during the apoptosis, but also the nature of quantum dots to resist photobleaching can benefit the use of them for longitudinal, dynamic monitoring under confocal microscopy. The photobleaching resistance of the GQDs capped with thiol-terminated molecules, in treated HeLa cells, was examined with a series of confocal laser microscopy measurements, as compared to that of SYTO, an organic fluorescent dye specific for nuclear staining (Figure 3). The exposure time for each image acquisition was 1 min, with the confocal laser (17.5 mW) scanning at 405 nm. The GQD photoluminescence intensity was relatively stable throughout the measurements, whereas the SYTO fluorescence intensity started to decay significantly after 10 min of imaging session. The intensity ratios of both GQDs and SYTO to their image backgrounds versus time were calculated and compared in Figure 3b. After 30 min of confocal laser scanning, GQDs maintained 80% of original photoluminescence intensity. In contrast, the SYTO underwent significant photobleaching and only kept less than 40% of initial fluorescence intensity.

For these STS-induced HeLa cell apoptosis studies (Figure 4a), we constructed several control groups by incubating HeLa cells with GQDs-NLS (column 1), GQDs-NES (column 2), GQDs-NES-linker-DEVD (column 3), and GQDs-NES-linker-DEVD-linker-NLS (column 4), for 1.5 h each. In the absence of STS, confocal microscopy revealed the control groups possessed no intracellular GQDs photoluminescence in columns 2 and 3, and approximately equal-distributions of GQDs within their cytoplasms and nuclei in columns 1 and 4. It indicates the NLS moiety of functional peptide is necessary for GQDs being internalized by cells. However, when HeLa cells were incubated with GQDs-NES-linker-DEVD-linker-NLS and then treated with STS at 0.1 and 4 $\mu$M for 1 and 4 h respectively, confocal microscopy showed significant decreases in GQD photoluminescence within nuclei (Figure 4a, columns 5 and 6). The average ratio of photoluminescence intensity per image pixel of a cell's nucleus ($I_{nucleus}$) to that of the cell ($I_{cell}$) decreased from about 1 in the controls to 0.7 (0.1 $\mu$M STS for 1 h) and 0.3 (4 $\mu$M STS for 4 h) after the apoptotic induction (Figure 4b). For better nucleus/cytoplasm contrast, nuclei of cells were stained red with the nuclear stain SYTO 59. Confocal microscopy of both SYTO-staining and GQD-SYTO colocalization revealed subcellular translocation of GQDs upon induction of apoptosis (Figure 4a, bottom column). The ratio of $I_{nucleus}/I_{cell}$ between the GQDs-NLS (column 1) and the GQDs-NES-linker-DEVD-linker-NLS (column 4), as illustrated in Figure 4b, decreased from approximately 1.2 to 0.95, suggesting that the proximally situated NES moiety of the functional peptide (column 4) acted as a modest counteragent to the nuclear

(37) Negishi, Y.; Nobusada, K.; Tsukuda, T. *J. Am. Chem. Soc.* **2005**, *127*, 5261–5270.
(38) Negishi, Y.; Takasugi, Y.; Sato, S.; Yao, H.; Kimura, K.; Tsukuda, T. *J. Phys. Chem. B* **2006**, *110*, 12218–12221.

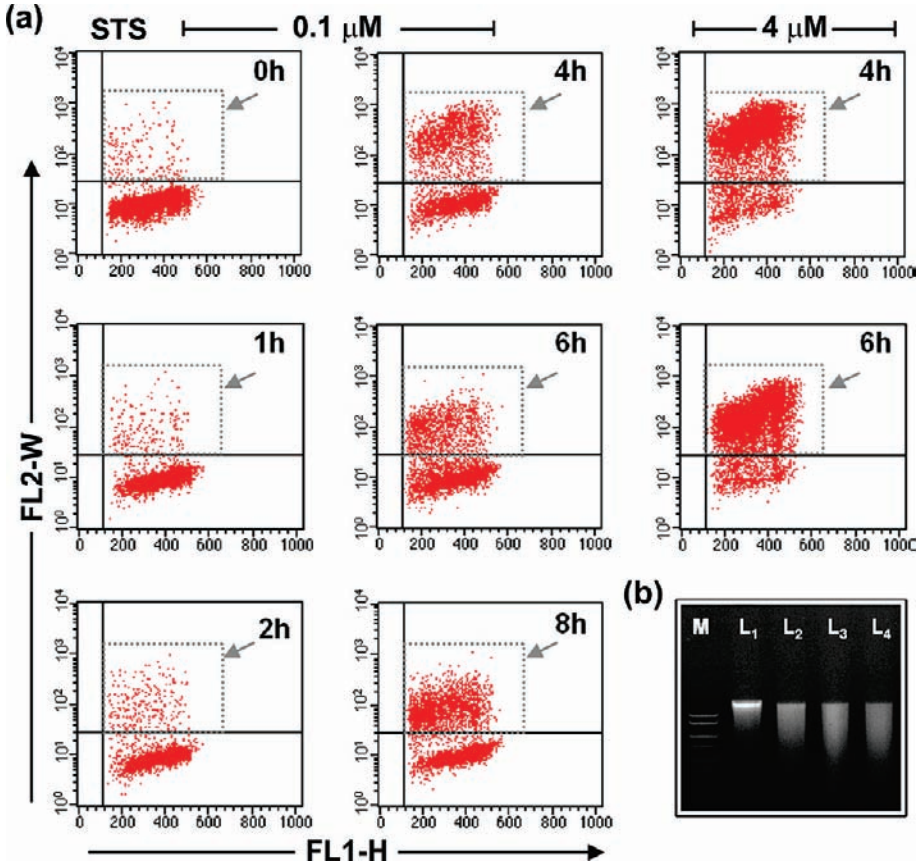


***Figure 6.*** (a) Population of apoptotic cells analyzed by flow cytometry under two conditions: 0.1 $\mu$M STS for 0, 1, 2, 4, 6, and 8 h; and 4 $\mu$M STS for 4 and 6 h. The *x*-axis and *y*-axis are dually stained with FITC-dUTP (channel 1, FL1-H: fluorescence pulse height) and propidium iodide (channel 2, FL2-W: fluorescence pulse width), respectively. The gray rectangle areas indicated by the gray arrows represent the population of apoptotic cells. The calculated apoptotic-cells ratios under treatments of 0.1 $\mu$M STS for 0, 1, 2, 4, 6, and 8 h are 2.3%, 4.2%, 8.5%, 41.8%, 28.4%, 50.3%, respectively; 4 $\mu$M STS for 4 and 6 h are 84.4% and 86.1% respectively. (b) Apoptosis-associated DNA-fragmentation was monitored by the DNA laddering assay, where M lane denotes markers (from top to down: 10 kDa, 8 kDa, 6 kDa, 5 kDa, 4 kDa, 3.5 kDa, 3 kDa, 2.5 kDa, 2 kDa, 1.5 kDa, 1 kDa, 750 bp, 500 bp and 250 bp) and $L_1$, $L_2$, $L_3$ and $L_4$ are indicative of 0, 2, 4, 6 h following the treatment of 4 $\mu$M STS, respectively.

targeting NLS moiety located more distally. On the other hand, following STS-induced cellular apoptosis, the $I_{nucleus}/I_{cell}$ ratio decreased significantly, indicating the predominance of GQDs exportation from nuclei. To further verify that the shuttle of GQDs is NES-dependent exportation, we constructed GQDs-random NES-DEVD-linker-NLS, in which the sequence of random NES (LQKKLEELEL) is rearranged from that of functional NES (LLLKKEEQLE). With the identical STS-treatment of column 6 (4 $\mu$M STS for 4 h), the HeLa cells incubated with GQDs-random NES-DEVD-linker-NLS revealed much less GQDs exportation from nuclei by confocal microscopy (Figure 4a, column 7 vs column 6) and its quantified ratio of $I_{nucleus}/I_{cell}$ (Figure 4b, ratio of column 7 vs ratio of column 6). The specificity of caspase-3 mediated signal with the reporter was further validated with the construct of GQDs-NES-linker-DEVG-linker-NLS, in which the DEVG was incorporated to replace the DEVD. The critical aspartic acid residue (D) in the caspase-3 cleavage site was substituted by a glycine residue (G), and the DEVG was reported with much less specificity to caspase-3 as compared to DEVD.[39,40] The HeLa cells incubated with the construct bearing DEVG illustrated inhibition of caspase-3 mediated GQDs exportation from nuclei (Figure 4a, column 8 vs column 6; and Figure 4b, ratio of column 8 vs ratio of column 6).

In the final stages of apoptotic induction, pro-caspase-3 (caspase-3 precursor; 32 kDa) is proteolytically activated to form the effector protease caspase-3 (17 kDa).[41] As shown by Western blotting in Figure 5a, STS (4 $\mu$M) induced the cleavage of pro-caspase-3 to activated caspase-3 in a time-dependent (and concentration-dependent) fashion, with the majority of activation occurring within 4 h of STS addition. Caspase-3 activity was measured using a caspase-3 specific enzymatic assay. As compared with the control, caspase-3 activity was found to be about 2- and 5-fold higher in cells treated for 4 h with 0.1 and 4 $\mu$M STS, respectively (Figure 5b). The period of maximal caspase-3 activity obtained from enzymatic assay was approximately 4 h following STS treatment (Figure 5b), consistent with that derived from real-time microscopy of functionalized GQDs (Figure 4). Similar results were obtained via flow cytometry by counting the number of apoptotic cells following STS treatment; with both 0.1 and 4 $\mu$M STS specimens exhibiting significant increases in apoptotic cell populations 4 h following STS addition (Figure 6a). Fragmentation of chromosomal DNA into multiples of 180 base-pair nucleosomal units, a hallmark of cellular apoptosis, was also observed in DNA

(39) Tyas, L.; Brophy, V. A.; Pope, A.; Rivett, A. J.; Tavare, J. M. *EMBO Rep.* **2000**, *1*, 266–270.
(40) Rehm, M.; Dubmann, H.; Janicke, R. U.; Tavare, J. M.; Kogel, D.; Prehn, J. H. M. *J. Biol. Chem.* **2002**, *277*, 24506–24514.
(41) Rehm, M.; Dussmann, H.; Janicke, R. U.; Tavare, J. M.; Kogel, D.; Prehn, J. H. M. *J. Biol. Chem.* **2002**, *277*, 24506–24514.

laddering assays (Figure 6b), further confirming the apoptotoic action of STS.

In summary, the subnanometer photoluminescent GQDs synthesized and subsequently functionalized with NES-linker-DEVD-linker-NLS peptides demonstrated activation of and transportation through the NPCs of living cells. The capsase-3 recognition sequence DEVD, placed within the NLS/NES peptide, served as a proteolytic site for activated form of the apoptotic protease caspase-3. As such, the NES-linker-DEVD-linker-NLS peptide enabled the GQDs to function as molecular probes for the real-time monitoring of cellular apoptosis.

**Acknowledgment.** This work was supported by grants from the National Nanoscience and Nanotechnology Program of National Science Council of Taiwan (NSC-96-2120-M-260-001) and from the National Health Research Institutes of Taiwan (NHRI-097-MED-PP-04 and NHRI-097-NM-PP-03). We thank Ms. Shu-Fen Hu, Ms. Hsin-Ying Huang and Ms. Chia-Wen Huang for acquiring confocal microscopic images and their invaluable support. Special appreciation is given to Dr. Jeffrey Souris of The University of Chicago, for his kind help in editing this work.

JA100561K